Real-Time Indirect Continuous Arterial Blood Pressure Measurements From ECG And PPG Waveforms Using Deep Learning

Hyo Chang Seo
University of Ulsan College of Medicine
Hyun Bin Kim
University of Ulsan College of Medicine
Gi-Byoung Nam
University of Ulsan College of Medicine
Min Soo Cho
University of Ulsan College of Medicine
Segyeong Joo (sgjoo@amc.seoul.kr)
University of Ulsan College of Medicine

Research Article

Keywords:

Posted Date: February 14th, 2022

DOI: https://doi.org/10.21203/rs.3.rs-1252661/v1

Real-time indirect continuous arterial blood pressure measurements from ECG and PPG waveforms using deep learning

Hyo Chang Seo[1†], Hyun Bin Kim[1†], Gi-Byoung Nam[2], Min Soo Cho[2], and Segyeong Joo[1,*]

[1] Department of Biomedical engineering, Asan Medical Institute of Convergence Science and Technology, Asan Medical Center, University of Ulsan College of Medicine, Seoul, Republic of Korea.
[2] Heart Institute, Asan Medical Center, University of Ulsan College of Medicine, Seoul, South Korea
*sgjoo@amc.seoul.kr

†These authors contributed equally to this work

Abstract

It is a well-known fact that it is important to accurately measure blood pressure. In particular, it is an even more important vital sign for the elderly and patients in hospitals. Non-invasive techniques for blood pressure measurement only afford discrete results. Although invasive measurement techniques overcome this issue and provide continuous results, they involve the risk of bleeding or infection and also cause discomfort to the patient. To address this issue, in this study, we developed a deep learning model that can estimate the arterial blood pressure (ABP) in real time using the waveform signals from electrocardiograms (ECGs) and photoplethysmograms (PPGs), without handcraft setting. Data pertaining to patients with various disorders admitted in the intensive care unit (necg, ppg= 1,126,870) were used. The performance of the model was evaluated (RSBP= 0.96, RMAP=0.92, and RDBP = 0.90) and verified to meet international standards. Even if the actual value changes dramatically, the estimated value shows a graph that follows the trend. Additionally, the ABP of patients with atrial fibrillation could be measured continuously and in real time.

Introduction

Arterial blood pressure (ABP) is one of the main vital signs in children as well as the elderly. With regard to hemodynamics, accurate measurements of the ABP can enable optimal intervention in unstable patients and play an important role in determining long-term perfusion. An abnormal blood pressure (BP), such as high or low BP, constitutes a major risk factor for cardiovascular disease (CVD) leading to heart attacks and can even cause blindness or cerebral apoplexy[1,2]. Thus, the ABP is recognized as an important parameter in intensive care unit (ICU) monitoring, and immediate treatment is administered if abnormal blood flows are detected. Furthermore, the continuous analyses of the BP of a patient in the ICU can potentially provide additional information regarding the patient's condition and also allow for the prediction of the rate of remission and mortality.

Generally, BP measurement techniques can be categorized as invasive or non-invasive methods. The standard non-invasive blood pressure (NIBP) measurement technique employs a cuff-based oscillometric method; this approach yields discrete systolic and diastolic blood pressure results. In invasive blood pressure (IBP) monitoring, a needle-type pressure sensor is inserted into the patient's artery to measure BP continuously and accurately; however, this approach involves the risk of infection and bleeding and also causes pain to the patient[3]. Consequently, considerable efforts have been devoted toward developing accurate algorithms for indirectly monitoring BP via non-invasive and continuous real-time measurements, in order to exploit the advantages of both of the above-discussed blood pressure measurement methods.

Thus far, many studies on the measurement of BP have focused on electrocardiograms (ECGs) and photoplethysmograms (PPGs), particularly the time interval of arterial pulses originating from the thoracic aorta to the peripheral sites. Using ECGs and PPGs, many cuff-less BP estimation methods based on parameters such as the pulse transit time (PTT), pulse wave velocity (PWV), and pulse arrival time (PAT) have been developed. Researchers have developed approaches for predicting BP by using methods based on signal processing techniques such as frequency analyses and linear and nonlinear regression methods[4-8]. Miao et al.[6] reported high-accuracy estimates of BP using the multivariate linear regression and support vector regression methods with various feature extensions, including the heart rate (HR) and PTT. Alghamdi et al.[4] proposed a novel hybrid method for predicting the systolic BP (SBP) and diastolic BP (DBP) using the Gaussian process regression method by extracting features such as the time, chaotic, and frequency regions.

Recently, BP has been estimated using artificial intelligence techniques, namely the recurrent neural network (RNN) based on the time series characteristics of ECGs and the convolutional neural network (CNN) based on characteristics of morphological pattern changes[9-14]. Miao et al.[13] combined the CNN and long-short term memory (LSTM) techniques to derive high-accuracy BP estimates using ECG signals, without handcrafted engineering. Back et al.[9] proposed a novel end-to-end technique based on a CNN, using the time and frequency domains of ECGs and PPGs to predict BP. However, most of these studies focused on subjects with a normal BP range and failed to consider patients with hypertension or hypotension. Furthermore, many previous studies were unable to realize BP predictions in real time with short-segment raw ECG and PPG data as the inputs. Consequently, further research should be devoted toward real-time measurements of the BP of patients with hypertension or hypotension; in general, this is also important for healthy people because it would enable faster detection of abnormal BP.

To this end, in this study, we developed a BP estimator employing deep learning for real-time, indirect, continuous ABP measurements using ECG and PPG waveforms, without handcraft. In addition, as the dataset was collected from ICU patients who suffered from various diseases, the developed model can estimate the BP of healthy people and also people with diseases. By combining a CNN and an RNN, the developed model focuses on the morphological properties of ECGs and PPGs and the time series properties, thus estimating the SBP and DBP of the input values, as illustrated in Fig. 1. We demonstrate that this algorithm enables real-time assessments of the ABP of ICU patients, without requiring cuffs or involving the pain and risks of invasive measurements.

Methods

Data acquisition and preprocessing The database contained raw ECG, PPG, and ABP signal values. Data from 980 patients were obtained from the MICU of the Seoul Asan Medical Center Hospital for critically ill patients between Apr 01, 2018 to May 31, 2019. This study was approved by the Institutional Review Board of the Seoul Asan Medical Center Hospital (IRB No. 2021-0833). This study was approved by the Institutional Review Board of the Seoul Asan Medical Center Hospital (IRB No. 2021-0833) and complied with the principles of the Declaration of Helsinki. There was no need to obtain prior consent from the patient according to the IRB criteria. SBP and DBP were measured by a GE B650 patient monitor and recorded every 2 s; since the initial 30 min was noisy, all biometric signal records used were collected after 30 min.
To equalize the ECG and PPG input lengths, the ECG data were downsampled to 60 Hz. Because ABP is a numerical value recorded every 2 s, ECG and PPG were also cropped for 2 s. We processed the inputted ECG and PPG, and SBP and DBP were output at the end of the signal. The data acquired were excluded three times in different ways to avoid overfitting and improve accuracy. First, patient data with noise or motion artifacts were excluded. Noise was visually identified and excluded, and the model was trained only with normal ECG and PPG signals. Second, as it is a commonly used normal and hypertension BP range criterion[15,16], we considered that the patient data were not available if the SBP was below 50 or above 200 because we aimed to estimate low BP values and BP values in the hypertension range. Finally, signals from all ICU patients were collected only once as data can be acquired multiple times per person and collection times vary from patient to patient. For data spanning less than 30 min, the values were removed from the final database, and for data spanning more than 3 h, the final part was removed. These data were normalized from -1 to 1 so that the scale for all data was similar. We preprocessed all the data using MATLAB. All processes are summarized in Fig. 2. A total of 1112700 recordings were obtained from 284 patients. The median follow-up available after each data was 2.3 (0.5–3) h. The mean and standard deviation were 127.93±22.93 and 67.03±14.41 for SBP and DBP, respectively.

Model We proposed a Resnet + Bi-LSTM model that could capture the time series and morphological features of ECG and PPG.
(i) Deep residual network (Resnet)
The CNN was first introduced by LeCun et al.[17] in 1989 to process images more effectively by applying filtering techniques to artificial neural networks. In 1998, LeCun et al.[18] proposed an CNN, which enabled effective extraction of various spatial features from images by stacking many network layers that are currently used in deep learning. However, studies have shown that the accuracy of results reduces with increased data and network depth; therefore, a residual block has been proposed to overcome these disadvantages[19]. The residual block was defined as shown in Fig. 3a. Here, x and H(x) are the input and output vectors of the block, respectively. By linking the output layer with information learned from the previous layer, the layer maps only the additional information that needs to be learned. In other words, as it is a system that preserves previously learned information and additionally learns new information, an accuracy of the same or a higher level is maintained without any compromises.

(ii) Long short-term memory (LSTM)
The RNN is a system for modeling sequence data; unlike other neural networks, it has a "hidden state."[20] Each time a new input is received, the network modifies the hidden state step by step so that the memories remaining are information that summarizes the entire sequence. However, the RNN has a long-term dependency problem when trying to exploit old historical information. A model that overcomes these shortcomings is the LSTM model, which can predict future data by considering historical data in a more macroscopic way. Fig. 3b shows the structure of the LSTM model, which is defined as follows.

$$f_t = \sigma(W_f \cdot [h_{t-1}, x_t] + b_f) \quad (1)$$
$$i_t = \sigma(W_i \cdot [h_{t-1}, x_t] + b_i) \quad (2)$$
$$\tilde{C}_t = tanh(W_C \cdot [h_{t-1}, x_t] + b_C) \quad (3)$$
$$C_t = f_t * C_{t-1} + i_t * \tilde{C}_t \quad (4)$$
$$o_t = \sigma(W_o \cdot [h_{t-1}, x_t] + b_o) \quad (5)$$
$$h_t = o_t * tanh(C_t) \quad (6)$$

where W stands for the weight parameter, b represents bias, and σ represents the sigmoid function, as mentioned in Fig. 3b. Forgetgate determines what value of the past cell state to erase considering the current input and the previous output. The input gate determines whether to store or discard the current information, as shown in Equations (1), (2), and (3). Then, a new cell state is updated as we have determined how much information to discard through forgetgate and how much information to add through the input gate, as shown in Equation (4). Subsequently, based on Equations (5) and (6), we determine the amount of the cell state value that is finally obtained and derive a new output value, h_t. In this work, we used the bi-directional LSTM (bi-LSTM), which minimizes the loss to the output value by adding an LSTM layer that handles backward to the existing LSTM layer[21].

(iii) Proposed Resnet + Bi-LSTM
As mentioned earlier, BP has temporal and spatial features of input signals, which are correlations between ECG and PPG's historical inputs. We utilized the morphological and time series properties of ECGs and PPGs as model features using a neural network with the Resnet + Bi-LSTM structure.
Input data (2×125) are inserted, followed by a residual block and Bi-LSTM; then, the estimated SBP and DBP are output. At this point, the ADAM optimization method is applied to the network with an initial learning rate of 0.001. The drop-out coefficient is 0.2 to ensure that learning is maintained properly. The network activation function used is a modified linear unit (ReLU) to address the gradient vanishing problem. In addition, L2 regularization is used to prevent overfitting of the model. We used Python in the Tensorflow framework for all these processes. Seventy percent of the preprocessed data were used for the training set, 10% for the validation set, and 20% for the test set.

Performance measurements In addition to SBP and DBP, the mean arterial pressure (MAP) was evaluated; it is defined as the average pressure of a patient's arteries during one cardiac cycle. MAP is strongly correlated with SBP and DBP and is effective at predicting the risk of CVD and other fatal diseases17-19. The actual MAP can only be determined by invasive monitoring and complex calculations; however, it can also be calculated using SBP and DBP using the following formula.

$$\text{MAP} = \frac{SBP+2(DBP)}{3} \quad (7)$$

The model's performance was evaluated using the MAE, RMSE, and MAPE values, which were calculated using the following equations.

$$\text{MAE} = \frac{1}{n}\sum_{i=1}^{n}(y_i - \hat{y}_i) \quad (8)$$

$$\text{RMSE} = \sqrt{\frac{1}{n}\sum_{i=1}^{n}(y_i - \hat{y}_i)} \quad (9)$$

$$\text{MAPE} = \frac{\sum_{i=1}^{n}\frac{y_i-\hat{y}_i}{y_i}}{n} * 100 \quad (10)$$

MAE is an indicator value that is averaged by converting the difference (error) between the actual value and the predicted value to an absolute value. RMSE is an indicator value that squares the error and divides it by n. MAPE is calculated by providing absolute values to the prediction error and expressing the prediction error as a percentage.

Results

Performance evaluation using deep learning model We implemented a Resnet + Bi-LSTM model using only the ECG and PPG signals and evaluated the performance of the model by comparing the measured BP value with the actual BP.

Fig. 4a, c, and e show the correlation plots comparing the actual and estimated values of the SBP, DBP, and MAP. Based on a comparison of the Pearson correlation coefficient (R) values, we confirmed a linear graph and a high correlation of 0.96 for the SBP, 0.90 for the DBP, and 0.92 for the MAP; in particular, the SBP values were found to be more accurate than the other BP values. Fig. 4b, d, and f show the Bland–Altman plots of the three BP values. As indicated on the right side of Fig. 4, the mean of the difference between the actual BP and the estimated BP values obtained using the proposed model is -0.04, 0.01, and -0.01 and the standard deviation of the difference is 6.30, 7.07, and 5.17 for the SBP, DBP, and MAP, respectively. The mean errors (MEs) are 5.06, 5.55, and 4.07, respectively. Table 1 lists the Pearson coefficient (R), the mean absolute error (MAE), root mean square error (RMSE), and mean absolute percentage error (MAPE) for the measured SBP, DBP, and MAP, as discussed in the Methods section.

Verification based on international standards for BP measurement When BP is measured using actual BP values, international standards exist to give validity and reliability for the measurement value. These criteria consist of independent protocols to verify the validity of a method.

(i) British Hypertension Society (BHS)

We prove that the BP values estimated using the proposed method with deep learning are in conformance with the BHS standard, as shown in Table 2. The BHS protocol uses grades A to D as criteria, and we calculated the percentages of the MAEs based on three groups: < 5 mmHg, < 10 mmHg, and < 15 mmHg. When the three criteria exceed 60%, 85%, and 95%, respectively, the results of the verification are considered to fall under grade A. The lower the percentage, the lower is the grade, i.e., from B to D. Our results indicate that the SBP and DBP obtained via the proposed method fall under grade B, while the MAP falls under grade A.

(ii) Association for the Advancement of Medical Instrumentation (AAMI)

We also prove that the BP values estimated using the proposed method with deep learning are in conformance with the AAMI standard, as shown in Table 3. The AAMI protocol requires a mean difference (MD) of 5 mmHg or less, a standard deviation (SD) of 8 mmHg or less, and 85 or more subjects. Our results show that the ME and STD values are -0.04 and 6.31 for the SBP and 0.01 and 7.07 for the DBP, which conform to the AAMI standard.

Evaluation of performance of the proposed model relative to that of previous approaches Table 4 presents a comparison of the proposed method with previous techniques for estimating BP using bio signals and deep learning techniques. Previous studies performed training based on the continuous BP, using the MAE and SD as evaluation metrics for the BP prediction accuracy.

Miao et al[13]., Eom et al[22]. , and Li et al[23]. estimated BP using at least two signals and reported performance results comparable to those of the proposed model. Unlike other studies, however, the proposed method can check the data output at intervals of 2 s in real time; hence, it is expected to be more useful in urgent situations, such as in clinical surgeries. Other studies have also reported NIBP monitoring; however, in this study, the BP at the arteries was directly measured via IBP monitoring, which is considered as the gold standard. Hence, the BP results are more accurate and have greater applicability. In addition, using clinical data instead of public data can help increase reliability, as the training involves more diverse patient groups. Furthermore, the proposed method affords shorter learning periods because processes such as feature extraction are not included.

BP estimation for patient with atrial fibrillation (AF) Hypertension is likely one of the major causes of AF[24]. Accurate measurements of the BP of AF patients are important, especially for the elderly, when treating hypertension with sudden elevations in the SBP or SBP exceeding 120 mmHg, which is associated with an increased risk of AF accidents[25-27]. The ECGs of the AF patient and normal patients exhibit visual differences in terms of the waveforms; the former may also involve features of invisible parts. Therefore, we estimated the BP of the AF patient using the singularities of deep learning that can learn such features.

The dataset used in this study comprised data pertaining to a total of 23 AF patients. Among these, two patients were excluded because they had motion artifacts or were data sets that were less than 30 min. Among the remaining 21 AF patients, the data of 14 patients were considered as the training set, the data of 3 patients were adopted as the validation set, and the data of the remaining 4 patients were considered as the test set, for

the purpose of confirming the performance of the proposed model in estimating the BP of AF patients. The total number of tests conducted was 18540.
The test results are presented in Fig. 5. We evaluated the estimates of the BP of the AF patients using existing performance evaluation methods. The MAE and SD values of the SBP, DBP, and MAP are 6.32 and 8.11, 7.21 and 7.98, and 5.59 and 6.94, respectively.

Calibration method for BP estimation Calibration is an important process for neural networks; it helps ensure that the predicted values of the model reflect the actual probabilities. Although accuracy is important when applying deep learning algorithms to real-world medical decision-making systems, it is also essential to clarify the incorrect predictions of the model. The proposed model does not require individual calibration. However, estimating ICU patients' BP necessitates more accurate values; therefore, the accuracy needs to be improved. One approach to achieve this is the calibration method, where the trained model is calibrated using partial data with short intervals for each individual, in order to improve the accuracy of the BP estimation.
Fig. 6 presents a comparison of the BP estimates obtained with and without calibration. The R values were higher after calibration (0.96, 0.92, and 0.96 for SBP, DBP, and MAP, respectively), and the MAE and SD values were 4.39 and 5.44, 4.65 and 5.75, and 3.38 and 4.32, respectively. Table 5 offers a comparison of the R, MAE, and SD values with and without calibration.

Discussion

In this work, we demonstrate that our proposed Resnet + Bi-LSTM model estimates IBP obtained in the ICU in compliance with international standards. Estimates of BP using ECG and PPG signals from patients with multiple diseases can indicate a variety of conditions. In particular, the ABPs estimated using deep learning in patients with AF or cardiogenic shock (CS) have not been investigated in previous studies. For AF, however, reliable ABP values have been obtained in terms of accuracy or other evaluation indicators. Based on this, we prove that blood pressure can be sufficiently estimated in patients with various diseases.
Fig. 7 shows the actual and estimated values of SBP, DBP, and MAP in three groups: AF patients, patients with normal ECGs having large BP variability, and patients with normal ECGs having small BP variability. The top three plots indicate that the estimated values follow a trend similar to that of the actual values, implying that our model can effectively estimate BP. The middle three plots compare BP values in patients with high variability. We can see that the estimated values are quite consistent with the actual values, even if they fall or rise by a large margin. For patients with AF (Fig. 7g, 5h, 5i), the estimates are not significantly consistent with the actual values compared to the top and middle plots; however, we can see that they follow their trend, which is considered to have been learned less owing to the lack of data available compared to normal patients.
Compared to other studies, our study has several strengths including reduced time segment lengths, wider range of BPs, and a large number of subjects. As mentioned earlier, IBP has more accurate values than NIBP and provides much more valuable information, such as CS initiation. We obtained IBP data from the hospital's ICU and conducted this study unlike conventional studies that have estimated NIBP using continuous BP values. Although there are no acceptable standard hypotension levels, SBP and DBP values below 90 and 60 mmHg, respectively, are recognized as hypotension, and clinically, hypotension is no less important than hypertension[28-30]. There are several studies that have estimated high BP[31], but only a few have estimated low-range BP, which makes our study novel. The SBP ranges from approximately 50 to 200 and DBP ranges from approximately 20 to 160; thus, it is possible to estimate BP using our method in cases of both hypertension and hypotension. Moreover, our study does not require any filtering or calibration of signals. This means that the proposed model does not require much time to learn data and estimate results, and because it does not need calibration, it is possible to produce results immediately without having to input values in advance for tens of seconds or even a few minutes. We evaluated the model's performance without a calibration-based method, but we also proved its performance with calibration. When calibrated, lower MAE and SD values and a higher R coefficient are achieved compared with the calibration-free method. This means that although some time is needed initially, more accurate BP values can be estimated, making it suitable for critical real-world clinical situations. Another advantage of our study lies in the amount of data. We used data of 284 intensive care patients cropped for 2 s. Thus, we were able to learn a lot more data compared to other studies. Therefore, not only does the bias decrease when learning, but the resulting accuracy also increases. Thus, BP estimation is possible in patients with various diseases.
Nevertheless, there are some limitations to our study. First, our study is limited to Asian mono-ethnic groups. Further external verification with multi-ethnic data is essential for our model to be used in clinical practice. Second, we conducted an experiment to estimate the BP of AF patients; however, we did not obtain reliable results owing to the lack of AF-related patient data compared to patients with normal ECG. However, as shown in Fig. 5, which presents an upward linear graph, such a limitation can likely be addressed by increasing the amount of AF patient data in the future.

Conclusion

We demonstrate and evaluate the performance of the proposed IBP estimation model using ECG and PPG. This technique allows patients with various diseases to estimate IBP only using ECG and PPG bio signals without the risk of infection and bleeding. In future research, the model can be trained using labeled data from more patients, enabling BP measurements for any patient.

Data availability

The data collected from the Asan hospital during this study are patient data obtained under the IRBs' ethical approval. The data that support the findings of this study are available from Asan hospital, but restrictions apply to the availability of these data, which were used under license for the current study, and so are not publicly available. Data are however available from the authors upon reasonable request and with permission of Asan hospital. The deep learning and related codes are available upon request by contacting the author at gusqlszld@naver.com.

References

1 Vasan, R. S. *et al.* Antecedent blood pressure and risk of cardiovascular disease: the Framingham Heart Study. *Circulation* **105**, 48-53 (2002).

2 Gu, D. *et al.* Blood pressure and risk of cardiovascular disease in Chinese men and women. *American journal of hypertension* **21**, 265-272 (2008).

3 Geddes, L. A. & Baker, L. E. *Principles of applied biomedical instrumentation*. (John Wiley & Sons, 1975).

4 Alghamdi, A. S., Polat, K., Alghoson, A., Alshdadi, A. A. & Abd El-Latif, A. A. Gaussian process regression (GPR) based non-invasive continuous blood pressure prediction method from cuff oscillometric signals. *Applied Acoustics* **164**, 107256 (2020).

5 Kachuee, M., Kiani, M. M., Mohammadzade, H. & Shabany, M. Cuffless blood pressure estimation algorithms for continuous health-care monitoring. *IEEE Transactions on Biomedical Engineering* **64**, 859-869 (2016).

6 Miao, F. *et al.* A novel continuous blood pressure estimation approach based on data mining techniques. *IEEE journal of biomedical and health informatics* **21**, 1730-1740 (2017).

7 Sharifi, I., Goudarzi, S. & Khodabakhshi, M. B. A novel dynamical approach in continuous cuffless blood pressure estimation based on ECG and PPG signals. *Artificial intelligence in medicine* **97**, 143-151 (2019).

8 Xing, X. & Sun, M. Optical blood pressure estimation with photoplethysmography and FFT-based neural networks. *Biomedical optics express* **7**, 3007-3020 (2016).

9 Baek, S., Jang, J. & Yoon, S. End-to-end blood pressure prediction via fully convolutional networks. *IEEE Access* **7**, 185458-185468 (2019).

10 Esmaelpoor, J., Moradi, M. H. & Kadkhodamohammadi, A. A multistage deep neural network model for blood pressure estimation using photoplethysmogram signals. *Computers in Biology and Medicine* **120**, 103719 (2020).

11 Lee, D. *et al.* Beat-to-beat continuous blood pressure estimation using bidirectional long short-term memory network. *Sensors* **21**, 96 (2021).

12 Lee, S. & Chang, J.-H. Oscillometric blood pressure estimation based on deep learning. *IEEE Transactions on Industrial Informatics* **13**, 461-472 (2016).

13 Miao, F. *et al.* Continuous blood pressure measurement from one-channel electrocardiogram signal using deep-learning techniques. *Artificial Intelligence in Medicine* **108**, 101919 (2020).

14 Panwar, M., Gautam, A., Biswas, D. & Acharyya, A. PP-Net: A deep learning framework for PPG-based blood pressure and heart rate estimation. *IEEE Sensors Journal* **20**, 10000-10011 (2020).

15 Whelton, P. K. & Carey, R. M. The 2017 clinical practice guideline for high blood pressure. *Jama* **318**, 2073-2074 (2017).

16 Whelton, P. K. *et al.* 2017 ACC/AHA/AAPA/ABC/ACPM/AGS/APhA/ASH/ASPC/NMA/PCNA guideline for the prevention, detection, evaluation, and management of high blood pressure in adults: a report of the American College of Cardiology/American Heart Association Task Force on Clinical Practice Guidelines. *Journal of the American College of Cardiology* **71**, e127-e248 (2018).

17 LeCun, Y. *et al.* Backpropagation applied to handwritten zip code recognition. *Neural computation* **1**, 541-551 (1989).

18 LeCun, Y., Bottou, L., Bengio, Y. & Haffner, P. Gradient-based learning applied to document recognition. *Proceedings of the IEEE* **86**, 2278-2324 (1998).

19 He, K., Zhang, X., Ren, S. & Sun, J. Proceedings of the IEEE conference on computer vision and pattern recognition. (2016).

20 Rumelhart, D. E., Hinton, G. E. & Williams, R. J. Learning representations by back-propagating errors. *nature* **323**, 533-536 (1986).

21 Schuster, M. & Paliwal, K. K. Bidirectional recurrent neural networks. *IEEE transactions on Signal Processing* **45**, 2673-2681 (1997).

22 Eom, H. *et al.* End-to-end deep learning architecture for continuous blood pressure estimation using attention mechanism. *Sensors* **20**, 2338 (2020).

23 Li, Y.-H., Harfiya, L. N., Purwandari, K. & Lin, Y.-D. Real-time cuffless continuous blood pressure estimation using deep learning model. *Sensors* **20**, 5606 (2020).

24 Psaty, B. M. *et al.* Incidence of and risk factors for atrial fibrillation in older adults. *Circulation* **96**, 2455-2461 (1997).

25 Clark, D. M., Plumb, V. J., Epstein, A. E. & Kay, G. N. Hemodynamic effects of an irregular sequence of ventricular cycle lengths during atrial fibrillation. *Journal of the American College of Cardiology* **30**, 1039-1045 (1997).

26 Sykes, D. *et al.* Measuring blood pressure in the elderly: does atrial fibrillation increase observer variability? *British Medical Journal* **300**, 162-163 (1990).

27 Thomas, M. *et al.* Blood pressure control and risk of incident atrial fibrillation. *American journal of hypertension* **21**, 1111-1116 (2008).

28 Gregory, A. *et al.* Intraoperative hypotension is associated with adverse clinical outcomes after noncardiac surgery. *Anesthesia & Analgesia* **132**, 1654-1665 (2021).

29 McDonald, C., Pearce, M., Kerr, S. R. & Newton, J. A prospective study of the association between orthostatic hypotension and falls: definition matters. *Age and ageing* **46**, 439-445 (2017).

30 Veronese, N. & Demurtas, J. in *Orthostatic Hypotension in Older Adults* 89-95 (Springer, 2021).

31 Socrates, T. *et al.* Improved agreement and diagnostic accuracy of a cuffless 24-h blood pressure measurement device in clinical practice. *Scientific reports* **11**, 1-9 (2021).

Acknowledgement
This work was supported by the National Research Foundation of Korea(NRF) grant funded by the Korea government(MSIT) (NRF-2021R1A2C1013755)

Author contributions
Hyo Chang Seo and HyunBin Kim trained the model,prepared the figures and/or tables, wrote the main manuscript, and preprocessed the database. Segyeong Joo reviewed the draft of the paper.

Competing interests
The authors declare no competing interests.

Table

Table 1. Performance results of proposed BP estimation model

	SBP	**DBP**	**MAP**
R	0.96	0.90	0.92
MAE	5.09	5.55	4.07
RMSE	6.33	7.07	5.16
MAPE	4.31	7.93	4.54

Table 2. Verification with BHS standard protocol

		Absolute difference			Grade
		≤ 5	≤ 10	≤ 15	
Proposed Model	SBP	56.5	88.6	98.5	B
	DBP	53.6	85.1	96.4	B
	MAP	67.9	94.7	99.3	A
BHS	Grade A	60%	85%	95%	
	Grade B	50%	75%	90%	
	Grade C	40%	65%	85%	

Table 3. Verification with AAMI standard protocol

		ME	**SD**	**Subjects**
Proposed model	SBP	-0.04	6.31	284
	DBP	0.01	7.07	
AAMI	SBP / DBP	≤ 5	≤ 8	≥ 85

Table 4. Compare the performance evaluation of the proposed model with that of other studies

Author	Model	Input data	SBP		DBP		MAP	
			MAE	SD	MAE	SD	MAE	SD
Ours	Resnet + Bi-LSTM	Raw ECG, PPG	5.06	6.31	5.55	7.07	4.07	5.17
Fen Miao et al	Resnet + LSTM	Raw ECG	7.10	9.99	4.61	6.29	4.66	6.36
H Eom et al	CNN + Bi-GRU	Raw ECG, PPG, BCG	4.06	4.04	3.33	3.42	-	-
YH Li et al	Resnet + Bi-LSTM	Featured ECG, PPG	6.73	14.51	2.52	6.44	-	-

Table 5. Comparison of model performance when calibration is free or based

	SBP			DBP			MAP		
	MAE	SD	R	MAE	SD	R	MAE	SD	R
Calibration	4.39	5.44	0.96	4.65	5.75	0.92	5.75	4.32	0.96
No calibration	5.09	6.30	0.96	5.55	7.07	0.90	4.07	5.17	0.92

Figure

Fig. 1. Flowchart of proposed model**.** Conv: convolutional layer; BN: batch normalization; LSTM: long short-term memory. Here, ECGs and PPGs are used as the input and the SBP and DBP are obtained as the output via two residual blocks and the Bi-LSTM. The two signals are filtered and applied to the model as inputs for 2 s.

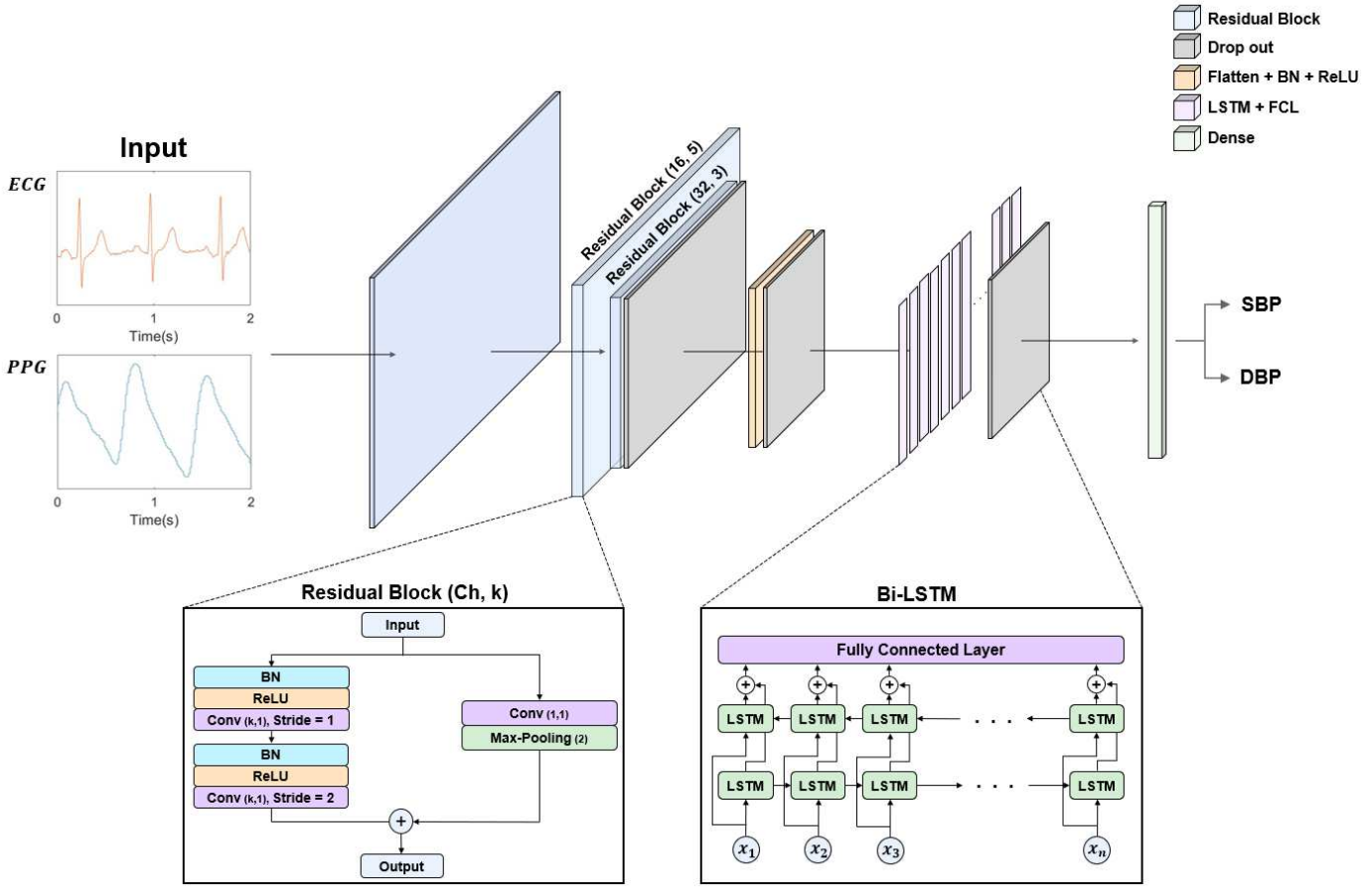

Fig. 2. Data preprocessing process and data split for deep learning. Data preprocessing and sorting are essential to improve learning accuracy. (a) To make the ECG the same length as the PPG, data were downsampled, denoised, normalized, and cropped for 2 s. (b)13 months of data from April 2018 to May 2019 were sorted; this included motion artifact removal and SBP range and data length adjustment. The final data consisted of training, test, and validation sets, with a corresponding ratio of 7:2:1.

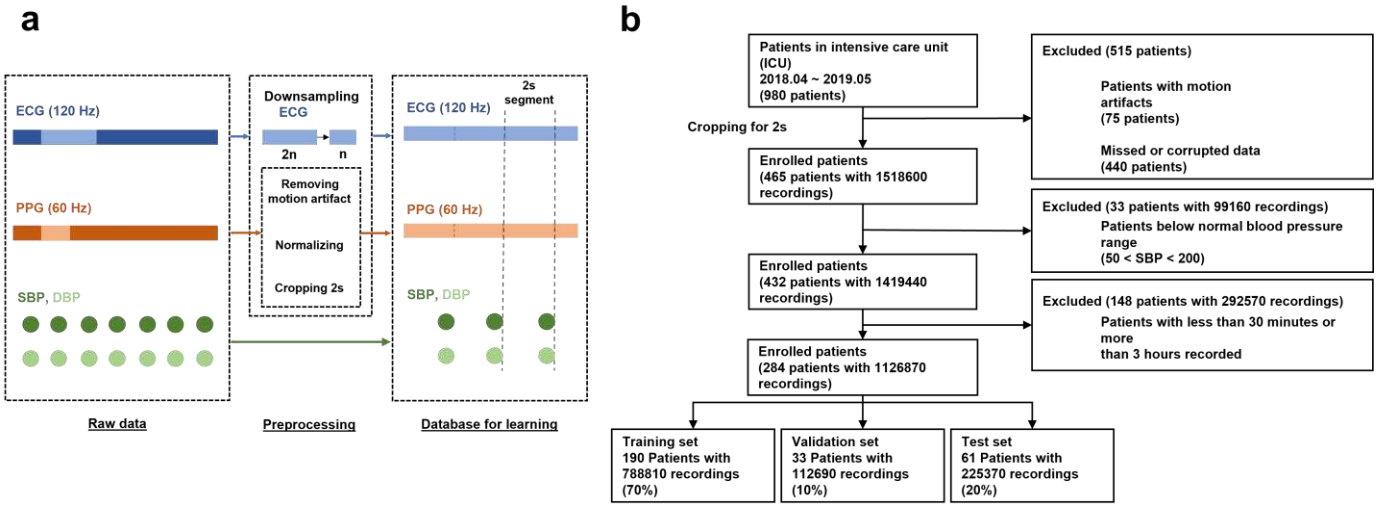

Fig. 3. Two main models for BP estimation. (a) Resnet's architecture makes deeper networks easier to learn than before by learning residuals. (b) The architecture of the LSTM enables learning by tuning existing and new information using cell and hidden state functions.

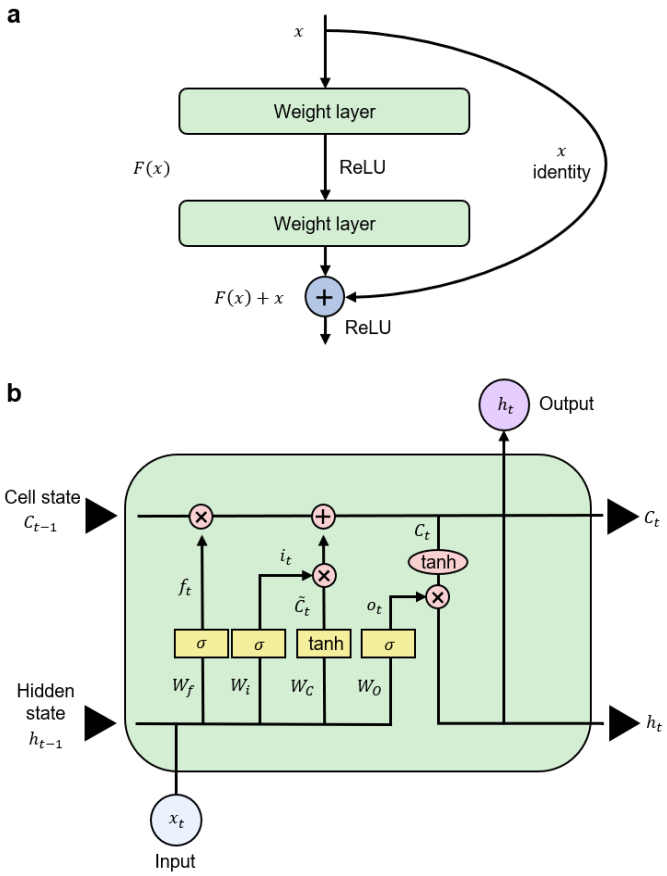

Fig. 4. Results of the correlation between actual and measured BP values. R: Pearson correlation coefficient, R; md: mean of the difference; sd: standard deviation of the difference. (a), (c), and (e) show the correlation plots for actual and estimated values of the SBP (R = 0.96), DBP (R = 0.90), and MAP (R = 0.92), respectively. (b), (d), and (f) show the Bland–Altman plots for actual and estimated values of the SBP, DBP, and MAP, respectively. The values of md and sd for (b), (d), and (e) are -0.04 and 6.30, 0.01 and 7.07, and -0.01 and 5.17, respectively.

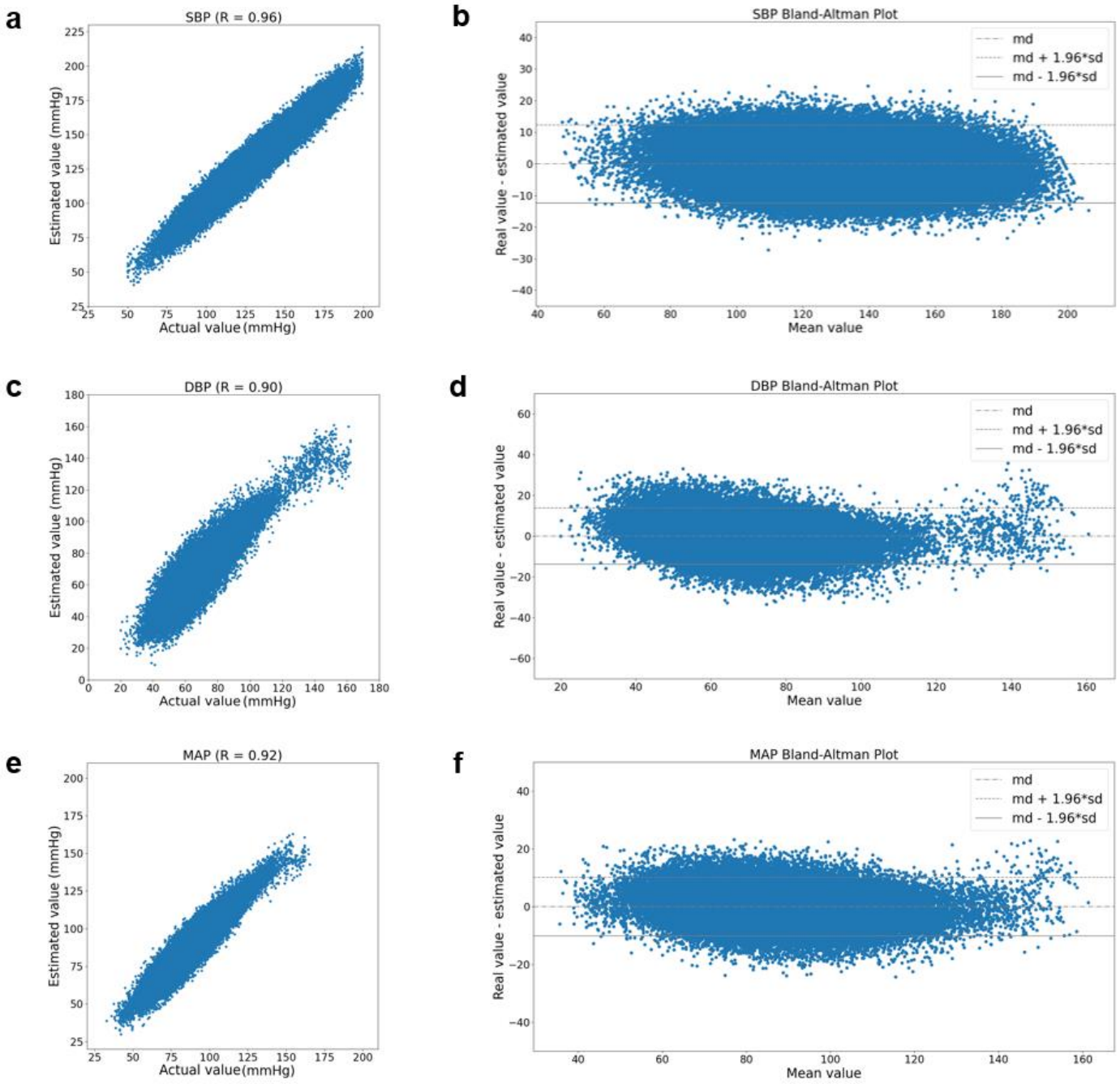

Fig. 5. Comparison of estimated BP of AF patients with actual values. The amount of data learned is 18540 with four patients. These plots exhibit tendencies similar to those of the ECGs of normal patients. From the left, the R values are 0.95, 0.87, and 0.92, respectively; these are somewhat lower than the results obtained when learning the entire dataset. The MAE and SD values are 6.32 and 8.11, 7.21 and 7.98, and 5.59 and 6.94, respectively, from the left; similar to the R values, these are also lower than the results when learning the entire dataset.

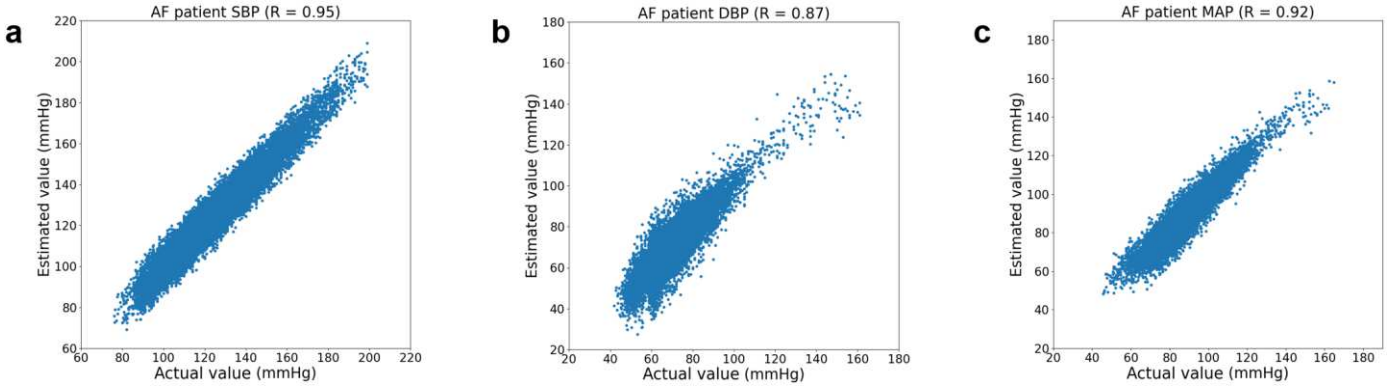

Fig. 6. Comparison of BP estimates with and without calibration. (a), (b), and (c) show the patient BP estimates without calibration in comparison with the actual values. (d), (e), and (f) show the patient BP estimates with calibration in comparison with the actual values. From the left, comparative graphs for SBP, DBP, and MAP, respectively, are shown; as is evident, calibration affords more accurate values, relative to the actual values.

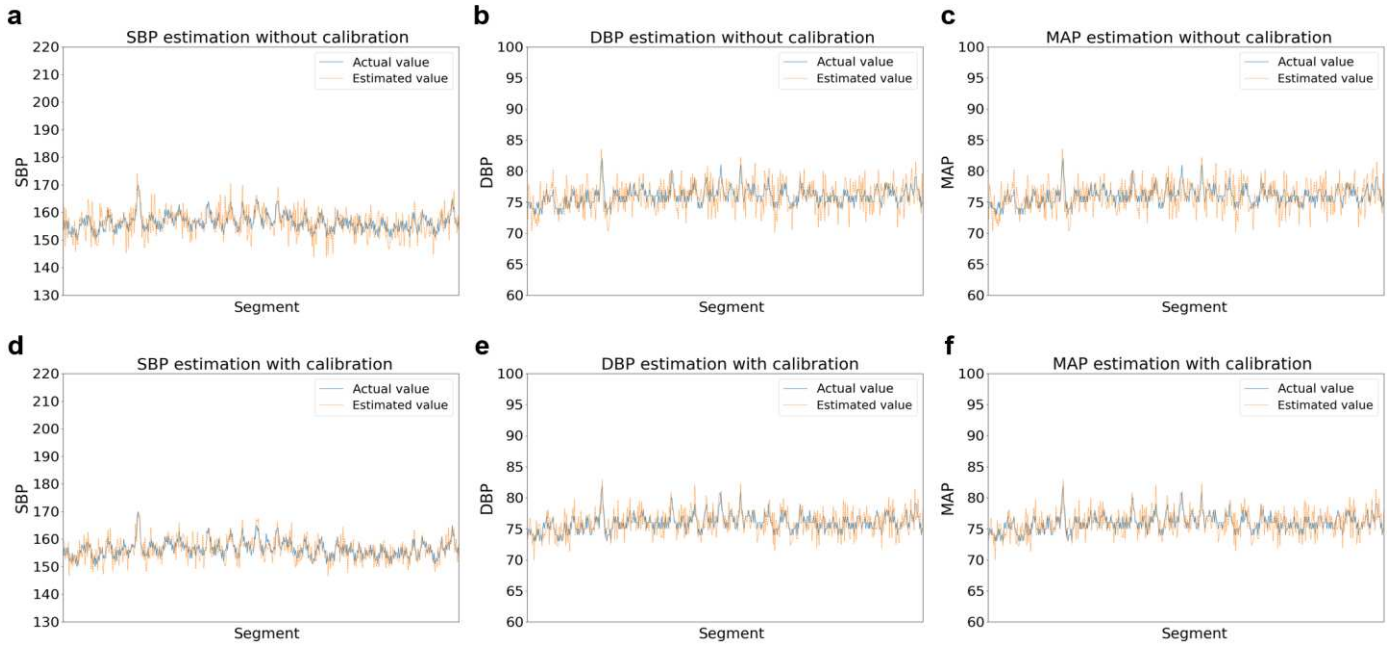

Fig. 7. Comparison of actual and estimated SBP, DBP, and MAP values. The blue lines represent the actual values, and the red lines represent the estimated values. (a), (b), (c) Comparisons of SBP, DBP, and MAP for patients with no significant variation in BP. The results indicate the good performance of our model, and the estimated values follow a trend similar to that of the actual values. (d), (e), (f) Comparison of SBP, DBP, and MAP for patients with large variations in BP. The results indicate that the estimated values follow a trend similar to that of the actual values. (g), (h), (i)Comparison of SBP, DBP, and MAP for patients with AF. Although the difference between the estimate and the actual value is slightly larger than that of a patient with a normal ECG signal, the graph shows similar results with the two values being proportional.